Curvelet Transform and Local Texture Based Image Forgery Detection

Muneer H. Al-Hammadi[1], Ghulam Muhammad[1], Muhammad Hussain[1], and George Bebis[2]

[1] College of Computer and Information Sciences, King Saud University, Riyadh, Saudi Arabia
Eng.muneer2008@gmail.com, {ghulam,mhussain}@ksu.edu.sa
[2] Department of Computer Science and Engineering, University of Nevada at Reno, USA
bebis@cse.unr.edu

Abstract. In this paper, image forgery detection method based on the curvelet transform and local binary pattern (LBP) is proposed. First, a color image is converted into the chrominance space. Then, the curvelet transform is applied to the chrominance component to decompose it into several scale and orientation wedges. The LBP normalized histogram is calculated from each of the wedges. The final feature vector is obtained by fusing all the histograms. The proposed method is evaluated on three image forgery datasets and compared with some state of the art methods. Experimental results demonstrate the superiority of the proposed method over the compared methods. The detection accuracy of the proposed method is 93.4% 97.0 % and 94.2% on the CASIA TIDE v1.0, CASIA TIDE v2.0 and Columbia color databases, respectively.

1 Introduction

The advancement of digital imaging technology increases the application of digital images in various aspects of our daily life, for example, newspaper, magazine, TV, commercials, security, insurance, to name a few. In one hand, the availability of low-cost and user friendly image editing tools make our life easier, and on the other hand, it raises a serious authentication issue due to its mishandling by some people. It has never been so easy to manipulate the images to gain illegal advantages or to make false propaganda using forged images [1]. Therefore, correctly detecting the forgeries in the images is a growing interest among the related researchers.

There are mainly two types of image forgeries, which are cloning and splicing. In the cloning forgery, a part of an image is copied and pasted to another part of the same image. In the image splicing, copy and pasting involve two or more images. The purpose of the image forgery is to duplicate or conceal a certain object into an image, or to make false propaganda. Performing of post-processing operations such as blurring, adding noise and JPEG compression or geometric operations such as scaling, shifting and rotation increases the hardness of the detection tasks.

The research on image forgery detection mainly started from early 2000. Many studies are reported on the literature to detect cloning forgery or splicing. Fridrich et al [2] and Huang et al [3] used discrete cosine transform coefficients to create a feature vector from the blocks of an image for block matching based methods of cloning forgery detection. Multi-resolution techniques, such as discrete wavelet

G. Bebis et al. (Eds.): ISVC 2013, Part II, LNCS 8034, pp. 503–512, 2013.

trans-form (DWT) is utilized in several methods [4], [5]. SIFT is another popular method in cloning forgery detection [6]. In image splicing detection, most of the works are evaluated using the Columbia authentic and spliced image dataset (color) [7] and CASIA tampered image detection evaluation dataset [8]. Ng et al used higher-order moments of the image spectrum to detect image splicing [9], while geometry invariants and camera response function are used in [10]. Shi et al proposed statistical features based on 1D and 2D moments, and transition probability features based on Markov chain in DCT domain for image splicing detection [11]. The method achieves 84.86% accuracy on the CASIA v2.0 database. Later, He et al improved the method by combining transition probability features in DCT and DWT domains [12]. For classification, they used support vector machine (SVM) - recursive feature elimination (RFE). Their method obtains 89.76% accuracy on the CASIA v2.0 database. The transition probability features extracted from chrominance channels of an edge-thresholded image was proposed in [13]. The method gets 95.6% accuracy in Cb chrominance channels in the CASIA v2.0 database, though in their experiments, they did not use the full database. The same method achieves 89.23% accuracy in Cb channel for Columbia color database. In another recent method, chroma-like channel is designed for image splicing detection [14], and improves the performance to 93.14% of the method [13] when applied to that chroma-like channel.

In this paper, an image forgery detection method based on a curvelet transform and local binary pattern is proposed. Curvelet transform is applied on chrominance components of a color image and LBP features are extracted from the resultant curvelet wedges. The LBP histograms of all the wedges are concatenated to form the feature vector. The SVM is used as the classifier. The main aim of this paper is to make a decision on image forgery, rather than localizing the forgery in the image.

The rest of this paper is organized as follows. In Section 2, the proposed method is described. Section 3 presents and discusses the experimental results, and section 4 concludes the paper with future work.

2 Proposed Method

Fig. 1 shows a block diagram of the proposed method. First, an RGB color image is converted into YCbCr chrominance space, where Y is the luminance, and Cb and Cr are the chrominance components. The Cb and Cr are the blue difference and the red difference, respectively. The human eyes is more sensitive to the luminance channel than the chrominance channels. As forgery is hard to detect in naked human eyes, chrominance channels are more suitable for forgery detection [13]. Therefore, the concentration is almost on Cb and Cr channels.

In the second step, the curvelet transform is applied to each individual chrominance component. Curvelet transform is a powerful multiscale multi-orientation image decomposition technique. It was developed to solve the problem of curve singularities. As an image analysis tool, it differs from other directional wavelet transforms in the degree of localization in orientation, which varies with scale. It provides a strong directional characterization in which elements are highly anisotropic at fine scales. With these properties, curvelet solve the isotropic and limited directional analysis of classic wavelet transform.

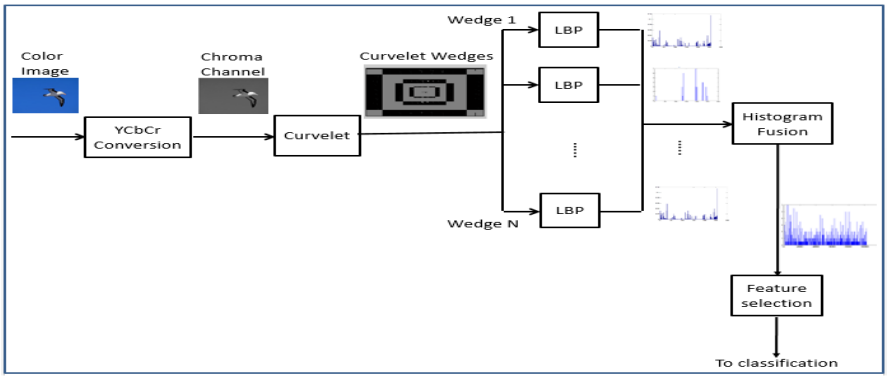

Fig. 1. Block diagram of the proposed curvelet and LBP based forgery detection system

The curvelet transform is actually an improvement for the ridgelet transform, which was proposed in 1999 as anisotropic geometric wavelet transform. The ridgelet transform can represent straight-line singularities perfectly. Unfortunately, global straight-line singularities rarely happen in real applications. The application of ridgelet transform on small partitions of the image to analyze local line or curve singularities, is the idea behind the curvelet transform proposed in 2000. A very efficient second-generation curvelet transform based on frequency partition technique was proposed after that [16]. To extract the curvelet coefficients, the corresponding image component (Y, Cb or Cr) is decomposed to different subbands of different frequencies. Then, each of these subbands is smoothly partitioned into squares of an appropriate scale. Each resulting square partition is renormalized to unit scale. The ridgelet transform is applied on each normalized partition. In this study, a 4 scales curvelet transform is used including the coarsest level. The second coarsest level is set to contain 8 different angles. The two higher frequency levels contain 16 different angles each and as a result we have a total number of 41 different angular wedges. Fig. 2 shows an example of a 3 scale curvelet transform and a total number of 25 curvelet wedges enclosed in the central square (the coarsest level) and different strips in the four Cartesian directions.

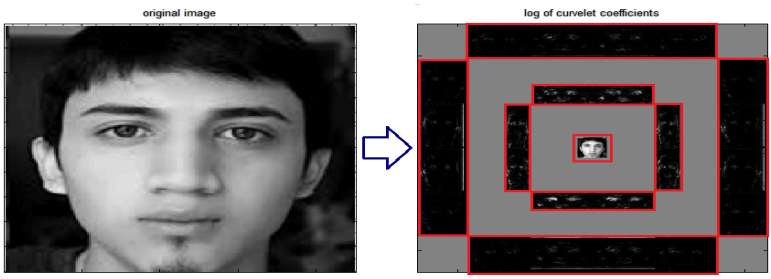

Fig. 2. Curvelet decomposition of an image in 3-scales and a total number of 25 curvelet wedges

The third step is the feature extraction, LBP is applied on each angular wedge of the curvelet to extract the LBP normalized histogram. LBP is a texture descriptor that labels each pixel in the image by thresholding the neighborhood pixels with the center pixel value and considering the result as a binary number as in Fig. 3. This type is called the basic LBP operator. Then the texture can be described by the histogram of these label values.

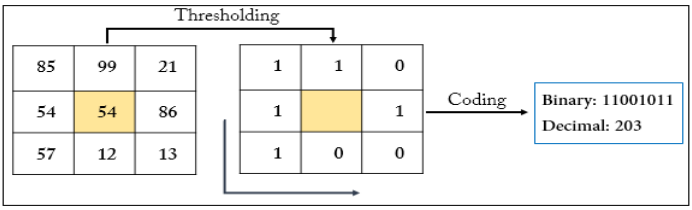

Fig. 3. The basic LBP operator

Another extension to the basic LBP operator is the uniform pattern in which only small subset of the total number of patterns is used to describe any texture. This subset of patterns is named uniform patterns. For any local binary pattern, it can be considered as uniform, if it contains at most two bitwise transitions from 0 to 1 or vice versa. For example, 00000000 (0 transitions), 11001111 (2 transitions) and 01110000 (2 transitions) are uniform, whereas 11001001 (4 transitions) and 01010010 (6 transitions) are not [17]. The length of the uniform LBP histogram of each wedge is 59 and as a result of histogram fusion, the resulting feature vector is of length 2419 (41 × 59).

While doing forgery, the original texture is distorted, and thereby, the LBP can encode texture differences at different scales and orientations of a curvelet transformed image.

In the fourth step, two different data reduction methods were used for feature selection, which are zero-norm minimization and local learning based (LLB) [18]. Zero-norm minimization ranks the features based on the statistical significance, while LLB removes features that contain redundant information. A cascading of the two methods is used to enhance the performance of the proposed method. In the cascading, first, zero-norm minimization is applied to select 50% of the total number of features (the most discriminative features). Then the LLB is applied on the selected features, and only those features having discriminative weight greater than the threshold of 10^{-10} according to LLB, are nominated. In the final step of the proposed method, the SVM classification with RBF (radial basis function) kernel and 10-fold cross-validation is used to evaluate the performance of the proposed method. Gamma and c parameters of the SVM are automatically set via a grid search process.

3 Experimental Results and Discussion

Three different datasets are used in our experiments, CASIA TIDE v1.0 [8], CASIA TIDE v2.0 [8], and DVMM images dataset of Columbia University [7]. Comparisons with other recent studies in the field of digital images forgery

detection are also provided on these datasets. In the experiments, a randomly selected 50% of the whole dataset samples are used for the feature selection step. The LIBSVM library [19] is then used for the classification. The optimal values for the parameters of kernel function and support vector classification (γ and c), are automatically set by an intensive grid search process using 25% of the whole dataset after reducing the number of features. The performance of the proposed method is given in terms of accuracy averaged over 10 iterations of the SVM. The accuracy is defined as:

$$Accuracy = \frac{TP+TN}{TP+TN+FN+FP} \times 100 . \quad (1)$$

where, True Positive (TP) is the number of forged images, which are classified as forged images, True Negative (TN) is the number of authentic images, which are classified as authentic images, False Positive (FP) is the number of authentic images, which are classified as forged images, and False Negative (FN) is the number of forged images, which are classified as authentic images.

Intensive experiments are carried out to test the performance of the proposed method. On different chrominance component with curvelet transform and LBP.

3.1 Experiments on CASIA TIDE v1.0 Dataset

CASIA TIDE v1.0 dataset contains a total number of 1721 images. 800 image are authentic and the remaining 921 are forged images of which 461 are cloned images and the remaining 460 are spliced. All the images have the size of 384×256 pixels, and they are in JPEG format.

3.1.1 Experimental Results on Cloned Images Subset of CASIA TIDE v1.0

The total number of images in this experiment is 719. The number of forged images are 461, and the rest are authentic images. Table 1 shows the averaged accuracies of the proposed method with and without feature selection in different chrominance channels on cloned images subset of CASIA TIDE v1.0 dataset.

Table 1. Results of the proposed method on cloned images subset of CASIA TIDE v1.0 dataset

Channels	W/O Feature Selection	With Feature Selection
Cb	88.5% ± 5.5	88.0% ± 3.9
Cr	90.0% ± 3.8	91.1% ± 3.3
Y	74.1% ± 6.8	79.4% ± 7.2
Gray	75.6% ± 4.9	78.5% ± 2.7

3.1.2 Experimental Results on Spliced Images Subset of CASIA TIDE v1.0

The total number of images in this experiment is 1082. The number of forged images are 460, and the rest are authentic images. Table 2 shows the averaged accuracies of the proposed method with and without feature selection in different chrominance channels on spliced images subset of CASIA TIDE v1.0 dataset.

Table 2. Results of the proposed method on spliced images subset of CASIA TIDE v1.0 dataset

Channels	W/O Feature Selection	With Feature Selection
Cb	92.5% ± 3.4	92.5% ± 3.3
Cr	92.8% ± 2.5	94.5% ± 1.8
Y	66.7% ± 5.0	67.4% ± 5.4
Gray	65.2% ± 4.8	68.7% ± 5.3

3.1.3 Experimental Results on the Whole CASIA TIDE v1.0 Dataset

The total number of images in this experiment is 1721. The number of forged images are 921, and the rest are authentic images. Table 3 shows the averaged accuracies of the proposed method with and without feature selection in different chrominance channels on the whole CASIA TIDE v1.0 dataset.

Table 3. Results of the proposed method on the whole CASIA TIDE v1.0 dataset

Channels	W/O Feature Selection	With Feature Selection
Cb	91.2% ± 2.0	90.7% ± 2.5
Cr	93.0% ± 1.8	93.4% ± 1.7
Y	67.6% ± 4.5	69.9% ± 3.0
Gray	67.8% ± 4.1	67.6% ± 3.3

The ROC curves in figure 4 illustrate the performance of the proposed method with and without feature selection on the whole CASIA TIDE v1.0, in different channels.

3.2 Experiments on CASIA TIDE v2.0 Dataset

CASIA TIDE v2.0 dataset contains a total number of 12614 images. 7491 image are authentic and the remaining 5123 are forged images of which 3300 are cloned images and the remaining 1823 are spliced. The image sizes varying from 240×160 to 900×600 pixels, and they are in JPEG BMP or TIFF formats.

3.2.1 Experimental Results on Cloned Images Subset of CASIA TIDE v2.0

The total number of images in this experiment is 5006. The number of forged images are 3300, and the rest are authentic images. Table 4 shows the averaged accuracies of the proposed method with and without feature selection in Cb and Cr channels on cloned images subset of CASIA TIDE v2.0 dataset.

Table 4. Results of the proposed method on cloned images subset of CASIA TIDE v2.0 dataset

Channels	W/O Feature Selection	With Feature Selection
Cb	95.2% ± 0.7	95.3% ± 1.2
Cr	95.0% ± 0.8	95.1% ± 0.7

3.2.2 Experimental Results on Spliced Images Subset of CASIA TIDE v2.0

The total number of images in this experiment is 3718. The number of forged images are 1823, and the rest are authentic images. Table 5 shows the averaged accuracies of the proposed method with and without feature selection in Cb and Cr channels on spliced images subset of CASIA TIDE v2.0 dataset.

Table 5. Results of the proposed method on spliced images subset of CASIA TIDE v2.0 dataset

Channels	W/O Feature Selection	With Feature Selection
Cb	93.9% ± 1.0	94.0% ± 1.0
Cr	94.5% ± 1.0	94.6% ± 1.2

3.2.3 Experimental Results on the Whole CASIA TIDE v2.0 Dataset

The total number of images in this experiment is 12614. The number of forged images are 5123, and the rest are authentic images. Table 6 shows the averaged accuracies of the proposed method with and without feature selection in Cb and Cr channels on the whole CASIA TIDE v2.0 dataset.

Table 6. Results of the proposed method on the whole CASIA TIDE v2.0 dataset

Channels	W/O Feature Selection	With Feature Selection
Cb	97.0% ± 0.5	96.8% ± 0.8
Cr	96.7% ± 0.5	96.6% ± 0.7

The ROC curves in figure 5 illustrate the performance of the proposed method with and without feature selection on the whole CASIA TIDE v2.0 dataset, in Cb and Cr channels

3.3 Experiments on DVMM Images Dataset

DVMM images dataset contains a total number of 363 images. 183 images are authentic and the remaining 180 are spliced images. The image sizes range from 757 × 568 to 1152 × 768 pixels, and they are in BMP or TIFF formats. Table 7 shows the averaged accuracies of the proposed method with and without feature selection in Cb and Cr channels on DVMM images dataset.

Table 7. Results of the proposed method on the DVMM images dataset

Channels	W/O Feature Selection	With Feature Selection
Cb	93.9% ± 5.0	94.2% ± 3.1
Cr	91.7% ± 5.9	92.8% ± 4.0

The ROC curves in figure 6 illustrate the performance of the proposed method with and without feature selection on the DVMM images dataset, in Cb and Cr channels.

For the purpose of comparison with other studies' performance, some of the recent researches, which are evaluated on the same datasets are selected. Table 8 shows the best accuracies achieved in each of those researches versus the accuracy achieved by the proposed method on both CASIA v2 and DVMM datasets. The proposed method outperforms all of those methods. The second highest accuracy achieved in [13], is 95.6%, but they did not use the full dataset.

CASIA TIDE v 2.0		DVMM	
Method	Accuracy	Method	Accuracy
[12]	89.8 %	[14]	93.1%
[13]	95.6%	[15]	85.0%
Proposed	97.0 %	Proposed	94.2 %

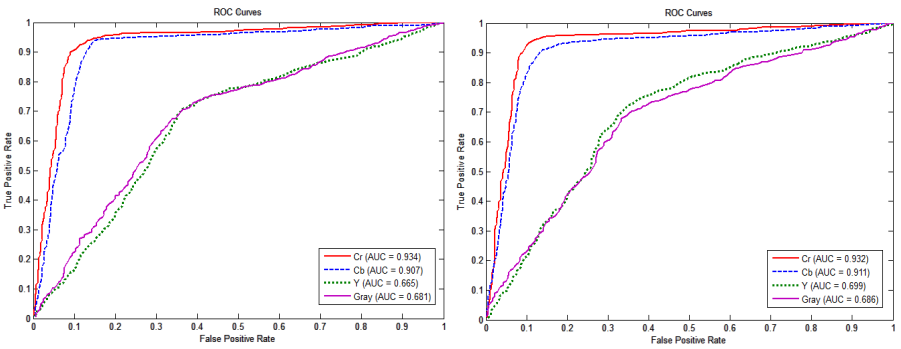

a) without feature selection b) with feature selection

Fig. 4. ROC curves of the proposed method on CASIA TIDE v1.0 dataset

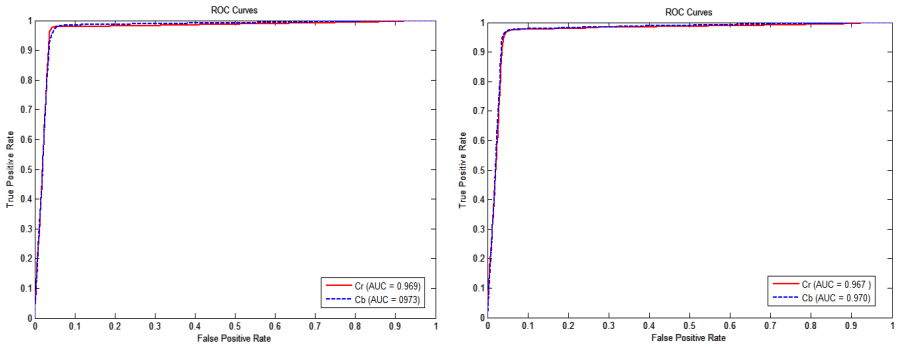

a) without feature selection b) with feature selection

Fig. 5. ROC curves of the proposed method on CASIA TIDE v2.0 dataset

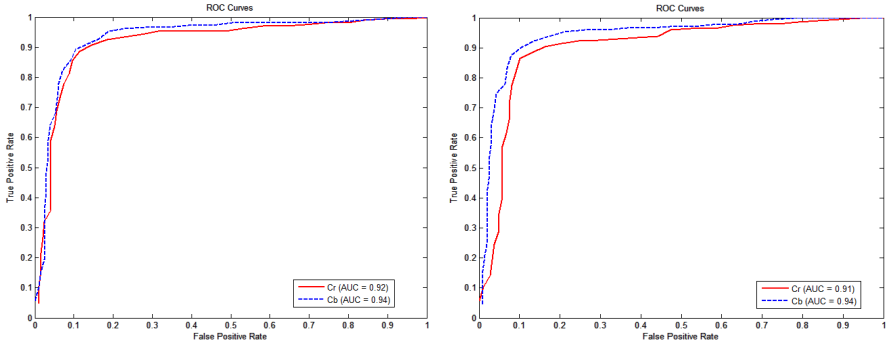

a) without feature selection b) with feature selection

Fig. 6. ROC curves of the proposed method on DVMM images dataset

4 Conclusion

A curvelet and LBP based image forgery detection method is proposed. The chrominance channels of an image are first transformed into multiple curvelet wedges of different scales and orientations. Then, LBP normalized histogram extracted from each wedges is used as features. SVM with RBF kernel is used as the classifier. Optional feature selection techniques are also applied. According to the experiments, the best accuracy is achieved in Cr and Cb chrominance components. The best accuracies of the proposed method are 91.74% on CASIA TIDE v1.0 dataset, 97.0% for CASIA TIDE v2.0 dataset, and 94.2% on DVMM images dataset. These accuracies are significantly higher than those obtained by the other state of the art methods on these datasets. Our future work will be to localize the forgery in the images.

Acknowledgement. This work is supported by the National Plan for Science and Technology, King Saud University, Riyadh, Saudi Arabia under project number 10-INF1140-02.

References

1. Swaminathan, A., Wu, W., Liu, K.J.R.: Digital Image Forensics via Intrinsic Fingerprints. IEEE Trans. Information Forensics and Security 3(1), 101–117 (2008)
2. Fridrich, J., Soukal, D., Lukas, J.: Detection of Copy-Move Forgery in Digital Images. In: Proceedings of Digital Forensic Research Workshop (August 2003)
3. Huang, Y., Lu, W., Sun, W., Long, D.: Improved DCT-based detection of copy-move forgery in images. Forensic Science International 206(1-3), 178–184 (2011)
4. Li, G., Wu, Q., Tu, D., Sun, S.: A Sorted Neighborhood Approach for Detecting Duplicated Regions in Image Forgeries based on DWT and SVD. In: IEEE International Conference on Multimedia and Expo, ICME 2007, Beijing, pp. 1750–1753 (2007)
5. Muhammad, G., Hussain, M., Bebis, G.: Passive copy move image forgery detection using undecimated dyadic wavelet transform. Digital Investigation 9(1), 49–57 (2012)
6. Amerini, I., Ballan, L., Caldelli, R., Del Bimbo, A., Serra, G.: A SIFT-based forensic method for copy-move attack detection and transformation recovery. IEEE Trans. Information Forensics and Security 6(3), 1099–1110 (2011)
7. Ng, T.T., Chang, S.F.: A dataset of authentic and spliced image blocks. Technical Report 203-2004, Columbia University (2004), `http://www.ee.columbia.edu/ln/dvmm/downloads/`
8. Dong, J., Wang, W.: CASIA tampered image detection evaluation (TIDE) database, v1.0 and v2.0 (2011), `http://forensics.idealtest.org/`
9. Ng, T.T., Chang, S.F., Sun, Q.: Blind detection of photomontage using higher order statistics. In: IEEE Intl. Symposium Circuits and Systems, ISCAS, pp. 688–691 (2004)
10. Hsu, Y.F., Chang, S.F.: Detecting image splicing using geometry invariants and camera characteristics consistency. In: IEEE ICME 2006, pp. 549–552 (2006)
11. Shi, Y.Q., Chen, C., Chen, W.: A natural image model approach to splicing detection. In: ACM Multimedia & Security, MM&S 2007, pp. 51–62 (2007)
12. He, Z., Lu, W., Sun, W., Huang, J.: Digital image splicing detection based on Markov features in DCT and DWT domain. Pattern Recognition (2012), `http://dx.doi.org/10.1016/j.patcog.2012.05.014`
13. Wang, W., Dong, J., Tan, T.: Image tampering detection based on stationary distribution of Markov chain. In: IEEE Intl. Conference on Image Processing, ICIP 2010, pp. 2101–2104 (2010)
14. Zhao, X., Li, S., Wang, S., Li, J., Yang, K.: Optimal chroma-like channel design for passive image splicing detection. EURASIP Journal on Advances in Signal Processing (2012), doi:10.1186/1687-6180-2012-240
15. Zhao, X., Li, J., Li, S., Wang, S.: Detecting digital image splicing in chroma spaces. In: Kim, H.-J., Shi, Y.Q., Barni, M. (eds.) IWDW 2010. LNCS, vol. 6526, pp. 12–22. Springer, Heidelberg (2011)
16. Starck, J.-L., Candès, E.J., Donoho, D.L.: The curvelet transform for image denoising. IEEE Transactions on Image Processing 11, 670–684 (2002)
17. Ahonen, T., Hadid, A., Pietikainen, M.: Face Description with Local Binary Patterns: Application to Face Recognition. IEEE Trans. Pattern Analysis and Machine Intelligence 28(12), 2037–2041 (2006)
18. Sun, Y., Todorovic, S., Goodison, S.: Local Learning Based Feature Selection for High Dimensional Data Analysis. IEEE Trans. Pattern Analysis and Machine Intelligence 32(9), 1610–1626 (2010)
19. Chang, C.C., Lin, C.J.: LIBSVM - a library for support vector machine (2010), `http://www.csie.ntu.edu.tw/~cjlin/libsvm`